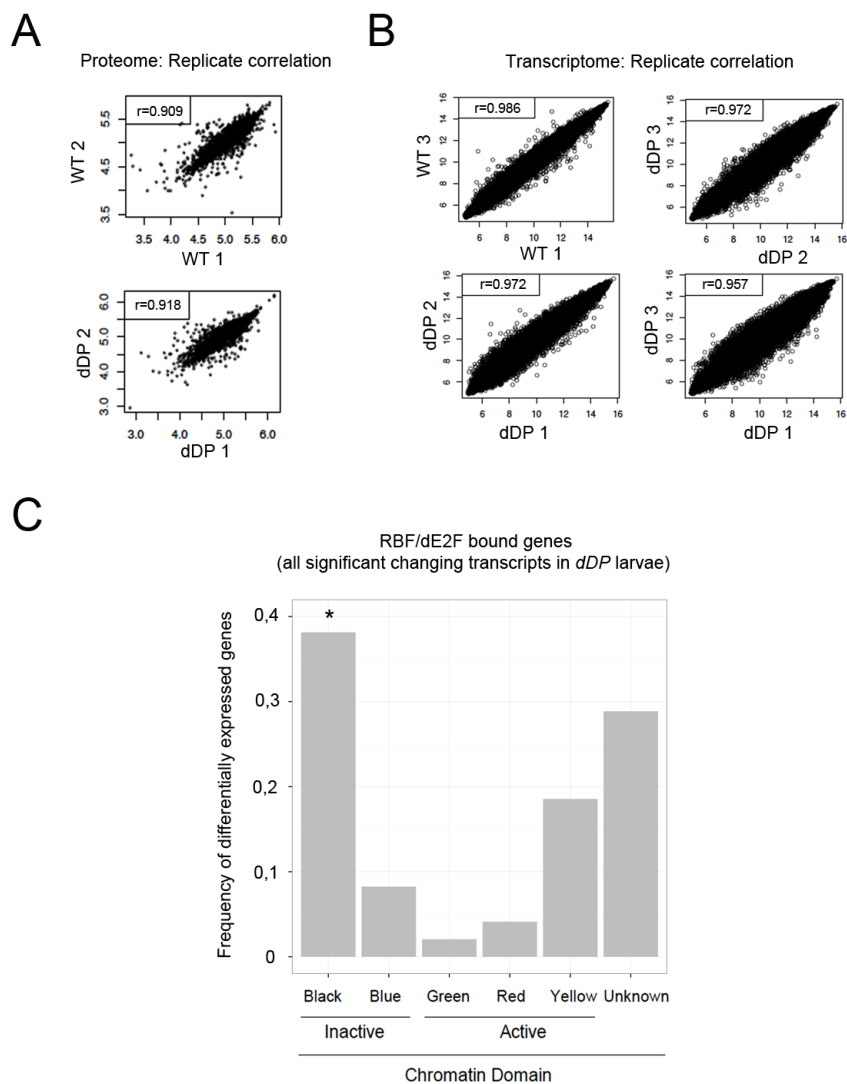
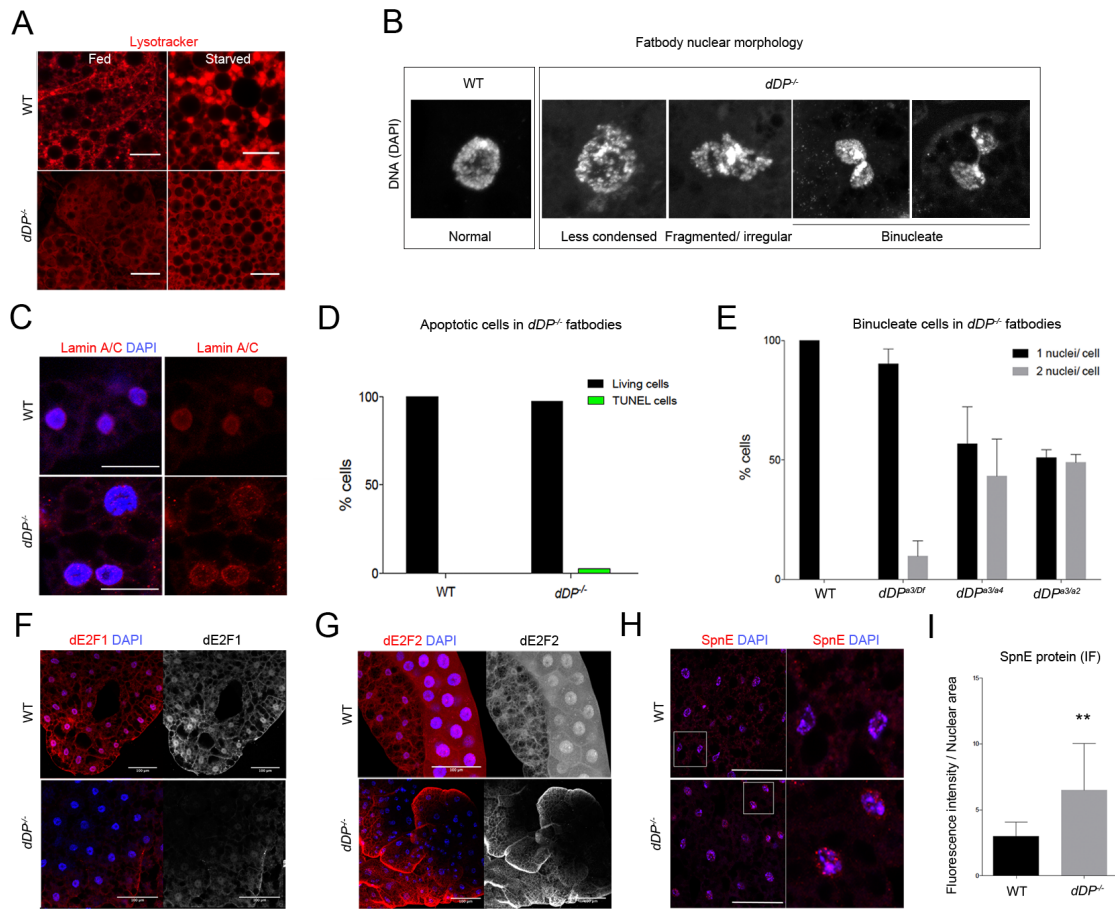


Figure S1



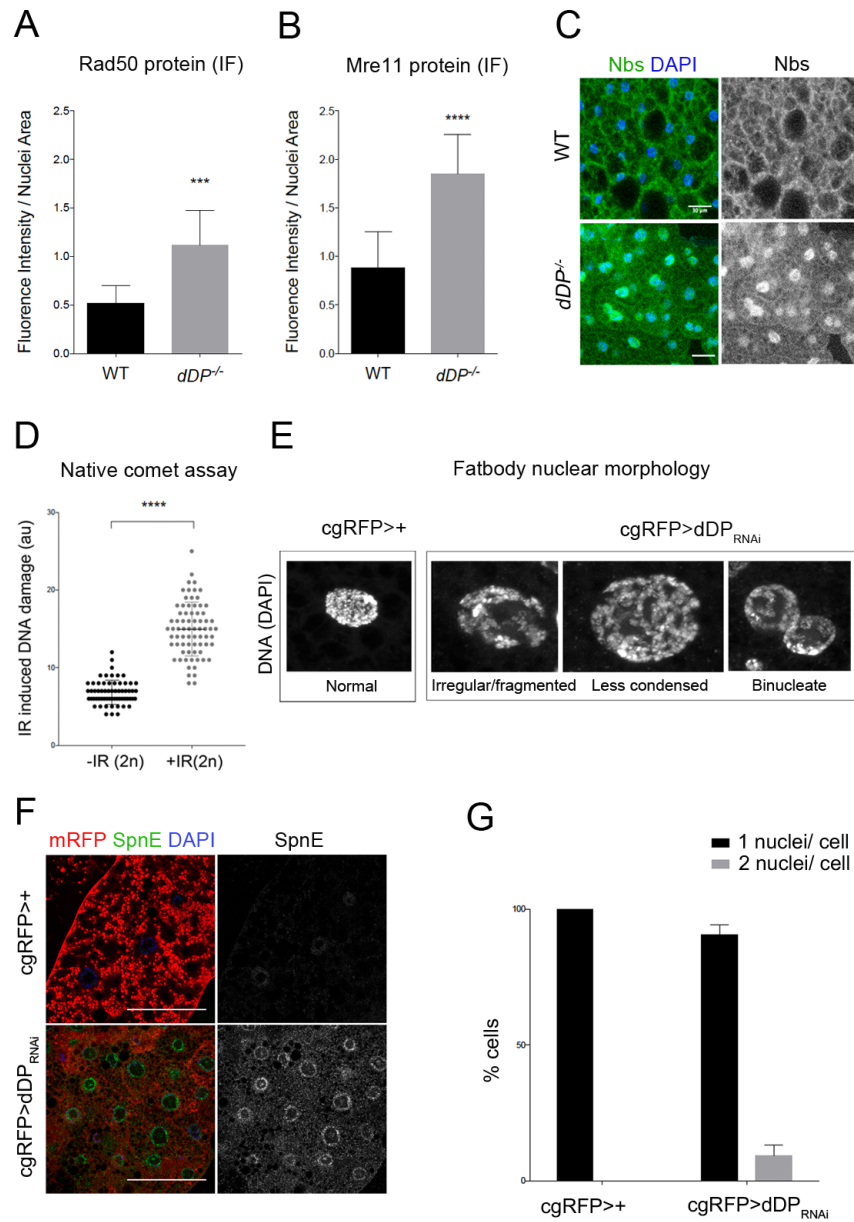
**Figure S1, related to Figure 1. Biological correlation of datasets and chromatin loci distribution of differentially expressed transcripts.** (A) Correlation plots between biological duplicates (proteome). (B) Correlation between transcriptome triplicates. (C) Frequency of chromatin localization of significant changing RBF/dE2F regulated loci to active/inactive domains (\* $p < 0.05$ ; Filion et al. 2010; data generated in *Kc* cells).

**Figure S2**



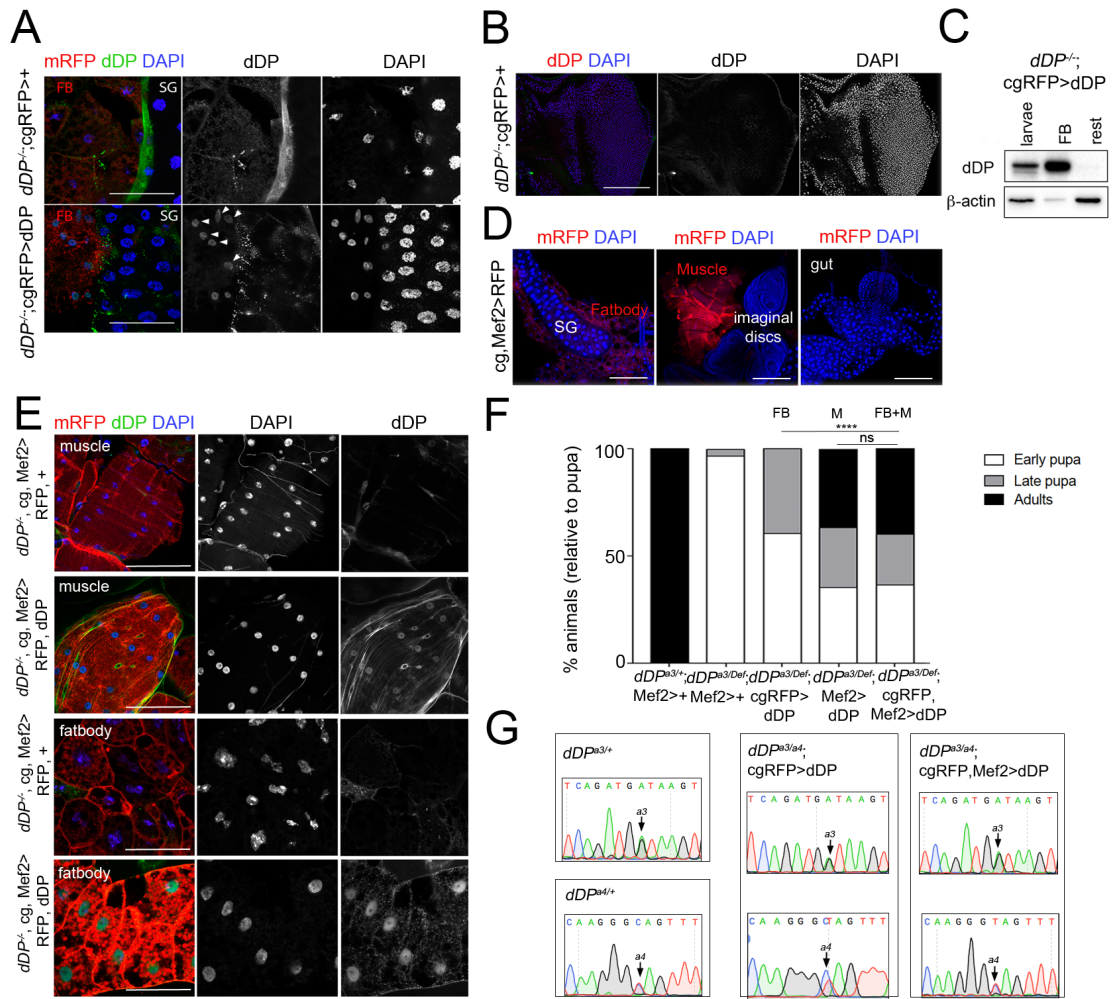
**Figure S2, related to Figure 2. Loss of E2F activity in fat body cells.** (A) Lysosomal vesicles in WT and *dDP*<sup>-/-</sup> fat bodies under normal and starvation conditions (scale bar, 20 μm). (B) Nuclear phenotypes in WT and *dDP*<sup>-/-</sup> fat bodies. (C) Lamin A/C is present in WT and *dDP*<sup>-/-</sup> fat body nuclei (scale bar, 30 μm). (D) TUNEL positive cells in WT (0%) and *dDP*<sup>-/-</sup> fat bodies (2.7%, n=37). (E) Mean ± SD % of binucleate cells in WT (n=60); *dDP*<sup>a3/Df</sup> (n=158); *dDP*<sup>a3/a2</sup> (n=110); *dDP*<sup>a3/a4</sup> (n=151). dE2F1 (F) and dE2F2 proteins (G) are absent in *dDP*<sup>-/-</sup> fat bodies (scale bar, 100 μm). (H) SpnE upregulation in *dDP*<sup>-/-</sup> FB cells (scale bar, 100 μm; mean ± SD of the intensity/nuclei area in I, unpaired t-test, \*\*p<0.01).

**Figure S3**



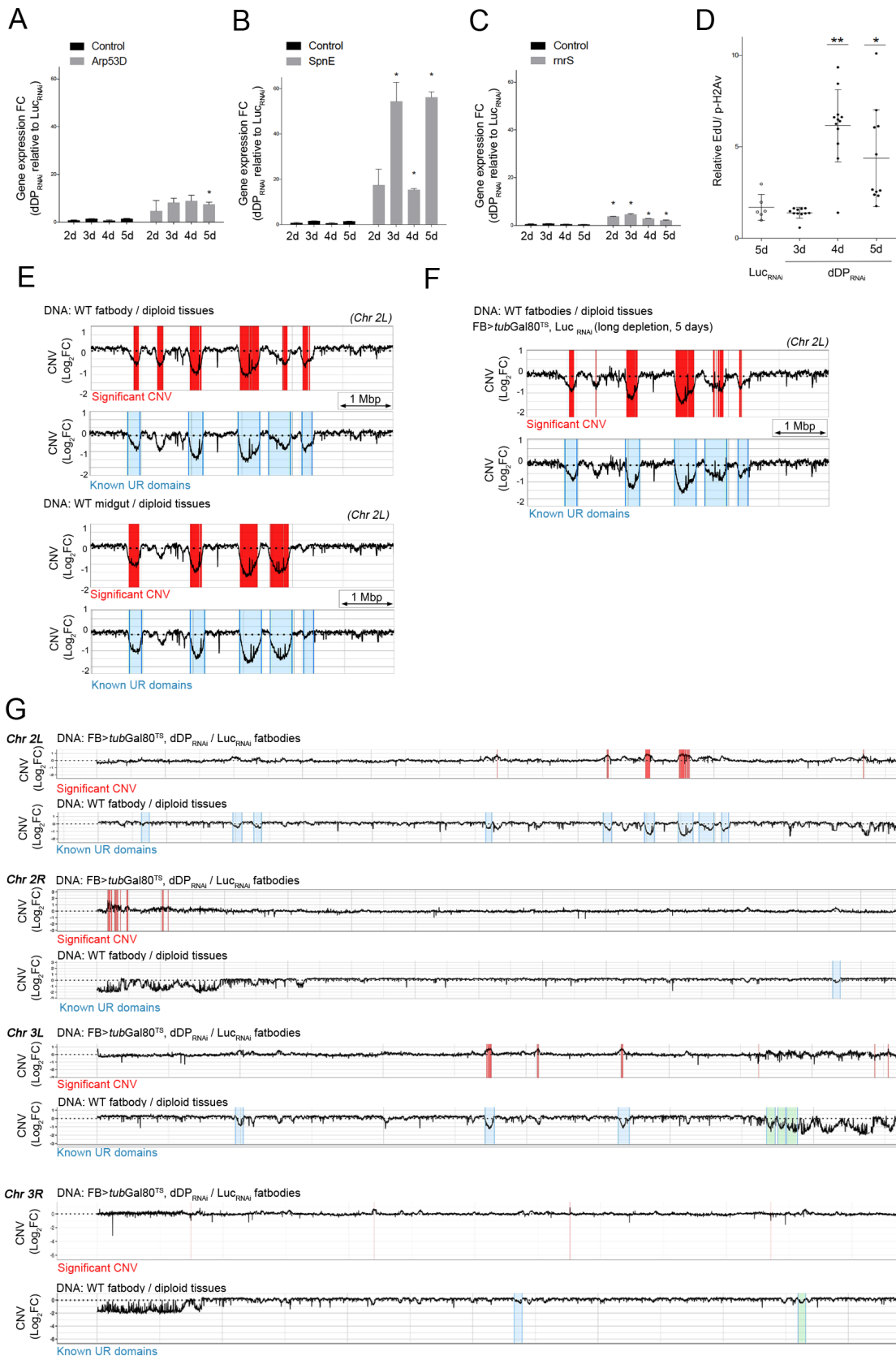
**Figure S3, related to Figure 3. DNA Damage activity is increased in dDP depleted fat body cells.** Rad50 (A) and Mre11(B) upregulation in *dDP*<sup>-/-</sup> fat body cells (mean  $\pm$  SD of the intensity/nuclei area; unpaired t-test, \*\*\*p-val<0.001 and \*\*\*\*p-val<0.0001 respectively). (C) Nbs protein is upregulated in *dDP*<sup>-/-</sup> fat bodies (scale bar, 30  $\mu$ m). (D) DNA damage induced in irradiated diploid cells (larval CNS, discs; IR, n=73; non-irradiated/-IR, n=62. Mann Whitney test, \*\*\*\*p-val<0.0001). (E) Nuclear morphology in cgRFP>+ and cgRFP>dDP<sub>RNAi</sub> fat bodies (F) Upregulated SpnE protein in cgRFP>dDP<sub>RNAi</sub> (control: cgRFP>+; scale bar, 100  $\mu$ m). (G) Mean  $\pm$  SD of the % of binucleated cells (cgRFP: n=300; cgRFP>dDP<sub>RNAi</sub>:n=330).

Figure S4



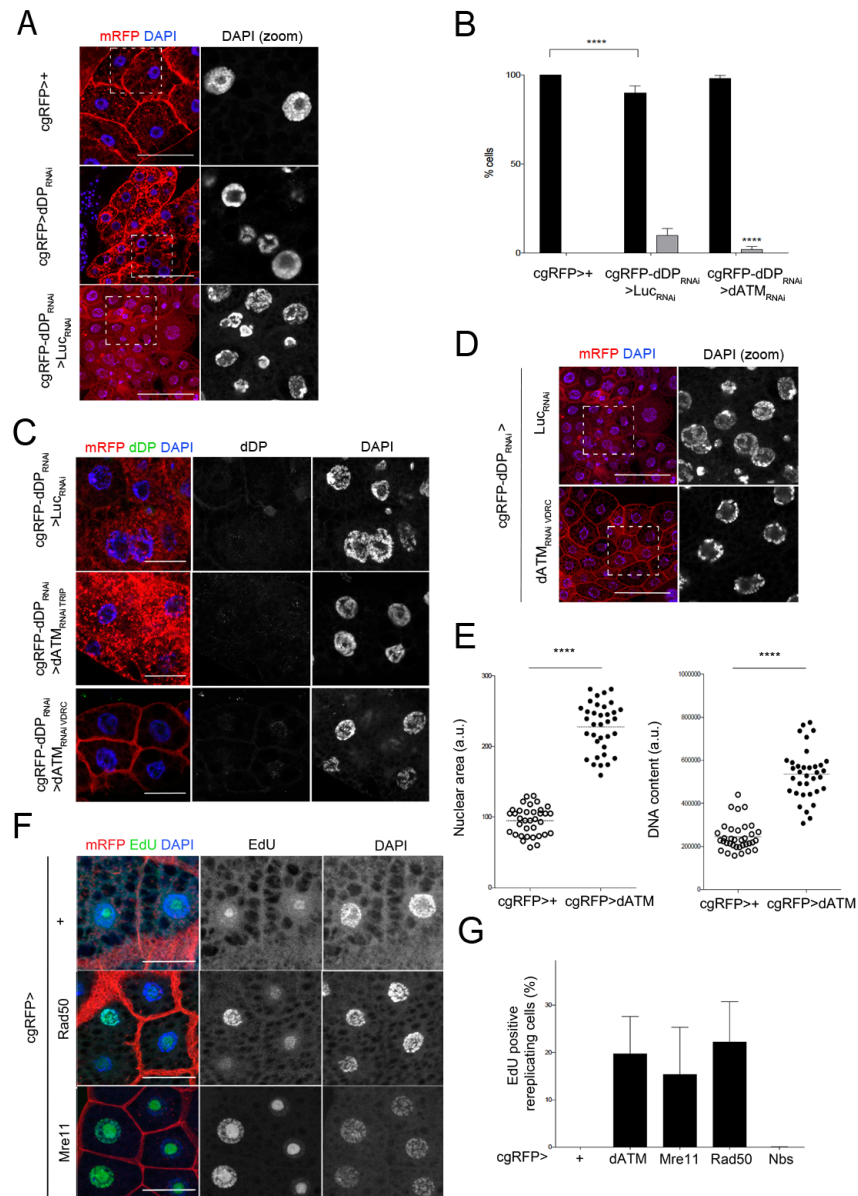
**Figure S4, related to Figure 4. dDP re-expression in fat body cells rescues *dDP* defects.** (A) dDP protein is specifically re-expressed in fat body cells of rescued animals (arrowheads; as control, adjacent salivary gland, SG; scale bars, 100  $\mu$ m). (B) Absent dDP protein in *dDP<sup>-/-</sup>;cgRFP>+* eye discs; scale bars, 100  $\mu$ m. (C) dDP blot of extracts from whole larvae, fat body and rest of larval tissues. (D) Combined expression of mRFP in muscles and fat body of *cgRFP;Mef2>+* larvae (absent in other tissues; SG, discs and gut; scale bars, 200  $\mu$ m). (E) dDP absence and re-expression in muscles and fat bodies of *dDP<sup>-/-</sup>;cgRFP;Mef2>+* and *dDP<sup>-/-</sup>;cgRFP;Mef2>dDP* (scale bars, 100  $\mu$ m). (F) % of animals arrested at each developmental stage: *dDP<sup>a3/+</sup>;Mef2>+* are viable; *dDP<sup>a3/Df</sup>;cgRFP;Mef2>+* developed 0% adults and 3.22% pharates. *dDP<sup>a3/Df</sup>;cgRFP>dDP* animals extended pupal development (39,32% pharates; n=178), and *dDP<sup>a3/Df</sup>;Mef2>dDP* animals resulted in 27.7 % of pharates and 36.6% of adults (n=90). Combined re-expression of dDP in fat body and muscles in *dDP<sup>a3/Df</sup>;cgRFP;Mef2>dDP* animals rescues more efficiently (n=30; 36.66% pupae, 23.33% pharates, 40% adults; Chi-squared test, \*\*\*\*p-val<0.0001 and ns, respectively). (G) Genotype of rescued animals and control mutant lines (*dDP<sup>a3</sup>* and *dDP<sup>a4</sup>* are point mutations described in Frolov et al., 2005).

Figure S5



**Figure S5, related to Figure 5. Time controlled depletion of dDP in the fat body results in DNA replication.** (A-C) Mean  $\pm$  SD gene expression fold changes of depressed dE2F target genes (Arp53D, SpnE and rnrS) in FB>*tubG80<sup>TS</sup>*>GFP, UAS>dDP<sub>RNAi</sub> fat body RNA (relative to UAS Luc<sub>RNAi</sub>; ANOVA, \*p-val<0.05). In black, the mean  $\pm$  SD of Gapdh and Rpl32 as control. (D) Relative EdU/p-H2Av signal quantification (n=10-12 nuclei/ time-point; Kruskal-Wallis, \*\*p<0.01 and \*p<0.05 respectively). (E) Inset of chromosome 2L: significant CNV (red) in WT fat body and midgut, relative to diploid tissues (known under-replicated (UR) domains, in blue). (F) Control depletion in FB>*tubG80<sup>TS</sup>*>GFP,UAS Luc<sub>RNAi</sub> fat bodies do not show replicating regions (significant CNV, in red) in known under-replicated regions (UR, blue). Genomic scale: 1 Million bp (Mbp). (G) significant replicating regions (in red) upon 5 days of dDP depletion in 2R, 2L and 3R, 3L chromosomes (CNV calculated between DNA of FB>*tubG80<sup>TS</sup>*>GFP, UAS dDP<sub>RNAi</sub> and UAS Luc<sub>RNAi</sub> in known under-replicated regions; Log<sub>2</sub>FC>0.6; FDR<0.001).

**Figure S6**



**Figure S6, related to Figure 6. dATM activity is critical in dDP depleted fat body cells.** In all cells, DNA is labeled with DAPI and mRFP is tagged to the membrane. (A) Nuclear defects of cgRFP>dDP<sub>RNAi</sub> (middle) are similar to the of cgRFP>dDP<sub>RNAi</sub>>Luc<sub>RNAi</sub> nuclei defects (control, cgRFP>+; scale bar, 100  $\mu$ m). (B) Mean  $\pm$  SD % of binucleate cells in cgRFP, cgRFP>dDP<sub>RNAi</sub>>Luc<sub>RNAi</sub>, cgRFP>dDP<sub>RNAi</sub>>dATM<sub>RNAi</sub> fat bodies (n= 100, 206, 262 cells respectively; ANOVA, \*\*\*\*pval<0.0001). (C) dDP protein is absent in cgRFP>dDP<sub>RNAi</sub>>Luc<sub>RNAi</sub> and cgRFP>dDP<sub>RNAi</sub>>dATM<sub>RNAi</sub> fat bodies (scale bar: 40  $\mu$ m). (D) An alternative UAS dATM<sub>RNAi</sub> (VDRc) line rescues nuclear defects (compare with cgRFP>dDP<sub>RNAi</sub>>Luc<sub>RNAi</sub>; scale bar, 100  $\mu$ m). (E) Individual plot measurements showing an increase in nuclear area (fold change= 2.42) and in DNA content (fold change= 2.01) of cgRFP>dATM cells (compared to control, cgRFP>+ nuclei, n=35; Mann-Whitney test, \*\*\*\*p<0.0001; au=airy units). (F) EdU in cgRFP>dRad50, Mre11 fat bodies (control, cgRFP>+; scale bar, 40  $\mu$ m). (G) Mean  $\pm$  SD of % EdU positive cells: cgRFP>dATM (19.74%), >Mre11 (15.41%), >Rad50 (22.21%), >Nbs (0.05%) (n=239, 260, 270, 500 cells, respectively).

**Figure S7**

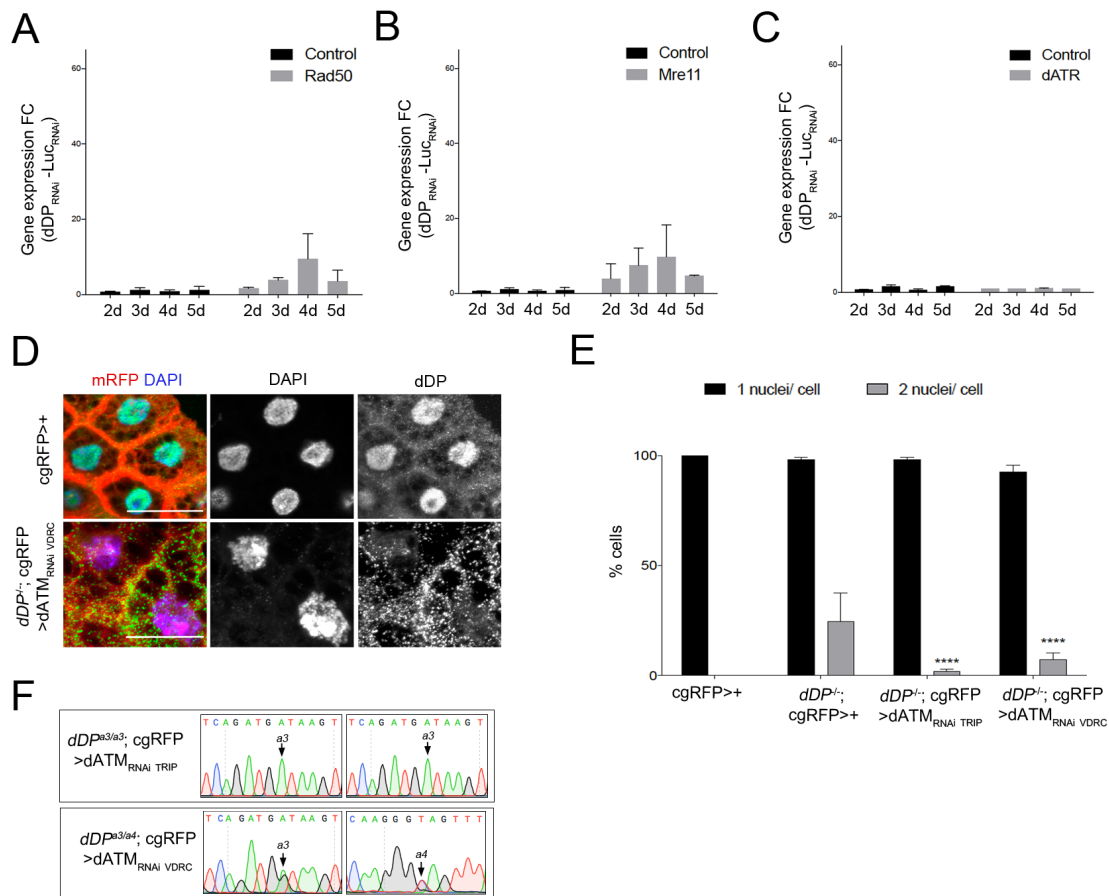


**Figure S7, related to Figure 7. Elimination of dATM rescues *dDP* phenotypes.** (A-C) Fold change in expression of Rad50 (A), Mre11 (B) and ATR (C) in *FB>tubG80<sup>TS</sup>>GFP, UAS>dDP<sub>RNAi</sub>* fat body RNA (compared to *UAS Luc<sub>RNAi</sub>*; *Gapdh* and *Rpl32* are used as control transcripts; ANOVA, ns). (D) Rescue of nuclear defects in the fat body of *dDP<sup>-/-</sup>; cgRFP>dATM<sub>RNAi</sub> (VDRC)* animals; scale bar, 25 μm. (E) Significant reduction of the mean ± SD of binucleate cells in both *dDP<sup>-/-</sup>; cgRFP>dATM<sub>RNAi</sub>* larvae (n= 100,147,267 and 199, respectively; ANOVA, \*\*\*\*pval<0.0001). (F) Genotype of *dDP<sup>-/-</sup>; cgRFP>dATM<sub>RNAi</sub>* animals (*dDP<sup>a3</sup>* and *dDP<sup>a4</sup>* are point mutations described in Frolov et al., 2005).



**Table S4**

<b>qPCR oligonucleotides</b>
tefu(F): GGGATTCGATAAACTGGC
tefu(R): AAAGGCAGCAGGCAGGTCTT
ATR(F): CCCTCTCTGGGAAGAATCGTG
ATR(R): CTTAACGCTCTCGTTGTC
Rad50(F): CGGAGTTTCGGCACCTATG
Rad50(R): TCTTTCCGCATCCGTTCTCG
Mre11(F): AACCAGTCGGTGAATTACGAGG
Mre11(R): CGTCGTGATTGCCATGAATAGAG
SpnE(F): TGATCGGCACCGACTATGTCA
SpnE(R): CTTGGCGTAGATGGACAAGTT
rnrS(F): CGTCCAAGGAAAACATTGCTG
rnrS(R): TGGTGCTATCCGTCAGAATCTT
Rpl32(F): AGCATAACAGGCCCAAGATCG
Rpl32(R): TGTTGTCGATACCCTTGGGC
Gapdh(F): TAAATTCGACTCGACTCACGGT
Gapdh(R): CTCCACCACATACTCGGCTC
<b>Genotyping primers</b>
Genotype (F): CCAGAACAAGTCCGAAATGG
Genotype (R): TGGTAAGAGGAGGATCACACG

**Table S4, related to STAR Methods.** All qPCR oligonucleotides are designed with FlyPrimerBank (Hu et al. 2013). Genotyping primers are described in Zappia and Frolov, 2016.